Challenging Glass 5 – Conference on Architectural and Structural Applications of Glass
Belis, Bos & Louter (Eds.), Ghent University, June 2016.

ISBN 978-90-825-2680-6

Numerical simulation of the EN 12600 Pendulum Test for Structural Glass

J. Pelfrene [a], S. Van Dam [a], J. Kuntsche [b], & W. Van Paepegem [a]
[a] *Ghent University, Department of Materials Science and Engineering, Belgium,*
[b] *TU Darmstadt, Institute of Structural Mechanics and Design, Germany,*
joren.pelfrene@UGent.be (J. Pelfrene)

In modern-day architecture, transparent glass units are omnipresent as large façades, windows, floors and balustrades. To ensure safety in an accident, glass panels must successfully pass the 'human impact' test, described by the international standard EN 12600. This test setup consists of a steel frame in which the test plate is clamped with prescribed force; and the pendulum impactor, hanging from a steel cable. The impactor weighs a total 50 kg and is built up from a rigid steel core to which two small tyres are mounted. The window panels are assigned a qualification number as they remain intact, fracture without losing integrity or fragment completely in impacts from different drop heights. As experimental testing is expensive and time-consuming, there is an interest in numerical modelling to predict a qualifying glass panel, which is already allowed by the German standard DIN 18008-4. Several modelling approaches allow the impact simulation for intact glass panels. This paper presents a detailed numerical model for the pendulum impact which enables realistic simulation of impactor, frame and test plate, to be valid also for the post-breakage safety assessment of laminated glass. The model shows good correspondence for static compression of the tyres and for impact against a pressure plate. Further comparison is made for the impact on a laminated glass panel that remains intact. Although less suited for structural design qualification, the detailed model can be used for future simulation of the post-breakage response of laminated glass panels.

Keywords: Safety Glass, Impact, EN12600, FEM

1. Introduction

Safety glass has been defined as glazing material which reduces the chance of injury upon accidental human impact. Severe and life threatening injuries may be caused by propulsion of sharp glass fragments or in penetration of a window pane. Other accidents may be caused by the collapse of a structural glass element, for example by failure of a glass balustrade or floor. For this reason, several qualification standards have been developed to assess safe response of a glass window when impacted by a human body at a certain speed.

In qualification of automotive windshield, it is common practice to closely mimic the most likely scenario by use of human-like objects. For assessment of human impact from inside the vehicle, crash test dummies are placed in the seats and the vehicle is propelled towards a rigid wall or another vehicle. In Europe, such tests are described by regulations ECE R-33 (1993) and ECE R-94 (2002). However, these regulations do not focus on the windshield, but collect data directly from a crash test dummy: acceleration of the head, tensile and shear forces at the neck/head interface and deflection between sternum and spine. Consequently, the entire inside of the car is evaluated: the windshield, but also the airbags, seatbelts, dashboard and steering column.

A testing method directly applicable to automotive windshield is described for pedestrian head impact EEVC (1998). A headform impactor, with accelerometer fitted inside, impacts the windshield with a prescribed speed of 40 km/h and at an angle of 65° with ground level. This testing method is not a required qualification standard, but is taken into account in the Euro NCAP safety rating system. This test has been the subject of study by Zhao et al. (2006), Timmel (2007), Liu et al. (2012) and Peng et al. (2013), who all use detailed finite element models of test dummies and pedestrian headform impactors for crashworthiness simulations. In such impact event, fracture of the windshield is beneficial in achieving lower accelerations experienced by the headform. Of course, the headform should not pierce the windshield and glass debris should be avoided as much as possible.

In construction, regulations regard the impact performance of the glass component directly, rather than the forces experienced by the impacting human body. In the past, the shotbag impact test (ANSI Z97.1, 1975) was accepted worldwide as a safety standard for window glass. This test method consists of a rigid clamping frame with internal width of 845 mm and internal height of 1911 mm and a 45 kg shotbag covered with a loosely draped cloth towel, proposed as a reasonable simulator for whole-body human impacts.

However, this test method received criticism for doubts over its reproducibility and changing characteristics of the shotbag over time, as demonstrated by Balkow et al. (1980). In Europe, the shotbag impactor has in the mean time been abandoned in favour of a twin-tyre impactor, as shown in Fig. 1, in the European norm EN 12600 (2002). This norm describes the impactor as a 50kg mass, consisting of a rigid deadweight surrounded by two tyres that are inflated to 3.5 bar. The test specimens have a size of 876 x 1938 mm and are clamped on all sides between 10 mm thick rubber linings that are compressed to 10%.

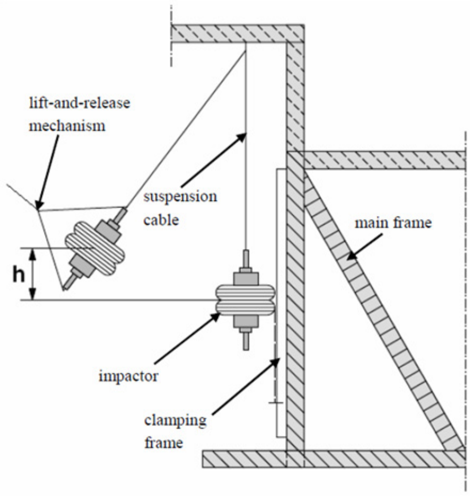

Fig. 1 Concept drawing of the pendulum impact test setup (EN 12600, 2002).

Qualification of glass setups by this test can become time-consuming and quite costly. Therefore, in Germany, the TRAV (2003) prescribed scantling for defined glass sizes and only required experimental testing with the twin-tyre impactor for deviating glass components. The most recent German norm DIN 18008-4 (2013) now also allows the calculation by either a simplified calculation or by numerical transient calculation for the geometry and support conditions of the final design. Leading up to this norm, several researchers have drafted validated numerical models for simulation of the impact up to glass breakage. In Schneider (2001), and also Müller de Vries (2012), the tyres are represented by volume-filling solid elements which are given a Young's modulus that corresponds to the observed stiffness of the tyre for a certain drop height. This approach receives the criticism that simulation results are matched rather than predicted and that they cannot be extrapolated to other glass setups than those for which the model has been validated. Brendler et al. (2004) and later Schneider et al. (2011) took account of the pressurized air volume in the tyres, but did not yet model the fibre reinforcement in the rubber. This paper introduces a numerical representation for the tyres with their actual material properties, which is to be more generally valid. Given the amount of experimental data that exists for this test, such model could further be used to compare and establish a reliable technique to simulate laminated safety glass into the post-fractured state. First, the model has to be verified for the impact on glass panels that remain intact for the entire duration of the test. This is discussed in Section 4, after introducing the tyre model and the comparison to experimental results for the impact against a pressure plate.

2. Numerical model of the tyres

The tyres used for the pendulum impactor in accordance with the European Standard EN 12600 (2002) are of the type STARCO TR13 ST11 3.50-8 PR4 with round section and flat longitudinal tread. These are bias-ply tyres for which the typical build-up is shown in Figure 2. The tyres consist of nylon body ply cords, rubber side wall and tread, and steel bead wires. The characteristics of the tyre, necessary for conceiving a numerical model, are not freely available. Therefore, experiments are conducted to look into the mechanical behaviour the tyre and its components.

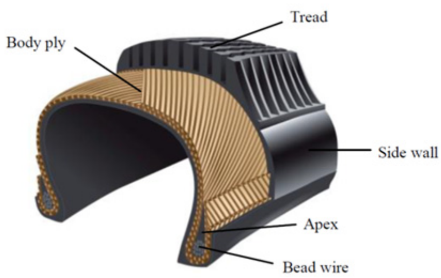

Fig. 2 Section sketch of a bias-ply tyre (Figure courtesy of ClassicTrucks.com).

2.1. Material properties

The nearly incompressible rubber material is best characterised by a hyperelastic material law, as large deformation can be expected. The measured Shore-A hardness of 59.5 roughly corresponds to Mooney-Rivlin constants C_{10} = 0.464 MPa and C_{01} = 0.116 MPa. The bulk modulus of rubber is typically about 2 GPa (Tabor, 1994). This initial estimation will prove to be sufficient, as the simulation results are relatively insensitive to perturbation of rubber material properties. More attention should be given to the nylon reinforcement cords which are placed in the tyre as two angled plies. Micro-CT imaging has been used on a cut-out section of the tyre to reconstruct the geometric configuration of the nylon plies in the rubber matrix. An image of the resulting 3D model is shown in Fig. 3.

The angle between two nylon cord layers is 60° and their diameter is 0.45 mm. The spacing between the individual nylon wires is 1.60 mm. To determine the Young modulus of the nylon PA6 cords, a tensile test is executed on a single nylon wire to obtain its stress-strain curve. Four samples were tested, showing a Young's modulus E = 1.39 GPa. The mechanical properties of the tyre materials are summarised in Table 1.

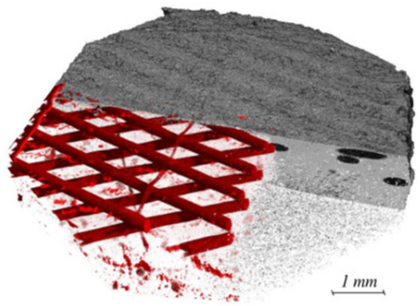

Fig. 3 Micro-CT image of a cut-out section of bias-ply tyre as used in the pendulum impact test: angled nylon plies in rubber matrix.

Table 1: Material properties for bias-ply tyre.

	Density	Stiffness	Poisson ratio
Steel	7850 kg/m³	E = 210 GPa	ν = 0.30
Nylon	1400 kg/m³	E = 1.39 GPa	ν = 0.30
Rubber	1100 kg/m³	C_{10} = 0.464 MPa C_{01} = 0.116 MPa K = 2.0 GPa	

2.2. Axisymmetric model: mounting and inflation

Numerical analysis of the double tyre pendulum impact is performed with the commercial finite element (FE) software ABAQUS, which offers some enhanced features for tyre modelling. In the first stage, an axisymmetric model of the tyre and rim is made to efficiently simulate mounting to the rim and inflation of the tyre. The resulting stress and displacement fields can then be extrapolated to a full 3D model for further analysis.

The geometry of a symmetric tyre section is drawn in its uninflated, unstressed state, as shown in Fig. 4a. This model is discretised by a finite element mesh of 931 axisymmetric elements, using continuum elements for both the rubber compound and the steel bead wires. Hybrid element formulation is used to prevent volumetric locking for the nearly incompressible rubber material; this formulation includes a hydrostatic stress distribution as additional unknown which must be calculated simultaneously with the displacements. The nylon cord plies can be modelled in ABAQUS by use of a rebar layer, embedded in the elements of the rubber compound (Korunovic, 2007). One rebar layer can represent multiple orthotropic reinforcement plies, of different materials, thickness, spacing and orientation. In the case of the bias-ply tyre, two equal nylon cord plies are assigned with orientations +30° and -30° with respect to the meridional direction.

Contact surfaces are defined between the tyre and the rigid rim to allow for frictional sliding during the mounting and inflation stages. An exact value of the frictional coefficient would be difficult to determine due to its dependency of several parameters (Sang, 2008), such as temperature, contact pressure, surface roughness, etc. For this reason, the frictional coefficient μ_f is estimated at 0.7. Figure 4b shows the simulated deformation after inflation to 3.5 bar, as prescribed by the standard EN 12600.

Additional simulations with $\mu_f = 0.5$ and $\mu_f = 0.9$ show that variation of the frictional coefficient has only a minor effect on the result. Only the displacement of nodes in the contact zone may vary in the order of 0.1 mm, while nodes away from the contact zone remain relatively unaffected.

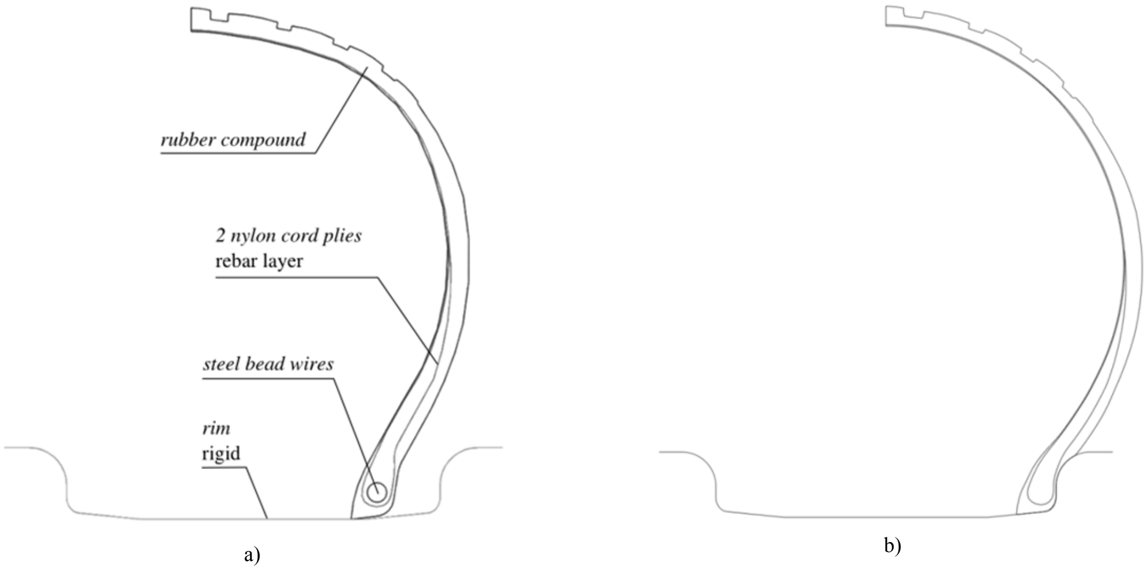

Fig. 4 Axisymmetric model of bias-ply tyre: a) Initial, unstressed state and b) after mounting and inflation

2.3. Detailed three-dimensional model

A detailed solid model is conceived through the symmetric model generation (SMG) option in ABAQUS. In essence, the SMG revolves the nodes of the axisymmetric model at regular offsets and connects them to form a 3D continuum elements mesh. The stress and deformation state of the mounting and inflation for the axisymmetric model can easily be transferred to the new 3D model. Three different levels of mesh refinement are studied, for which the characteristics are given in Table 2.

For simulation of the impact event using an explicit solving scheme, a more efficient 3D model is preferred. This model is constructed using shell elements with rebar layers defined for the nylon cord plies and the steel bead wires. The shell element thickness is taken to be constant as the sidewall thickness measured on the tyre, i.e. 3.0 mm. Further simplification is required for the implementation of the rebar layers; see Figure 5. Two rebar layers are defined for the nylon cord plies, each at a constant offset from the shell middle surface. An extra rebar layer for the steel bead wires is placed near the inner diameter of the tyre, with 9 wires of 1.0 mm in thickness each.

For this model as well, three different levels of mesh refinement are studied. The element length is refined in both meridional and concentric directions. Characteristics of the meshes are given in Table 2.

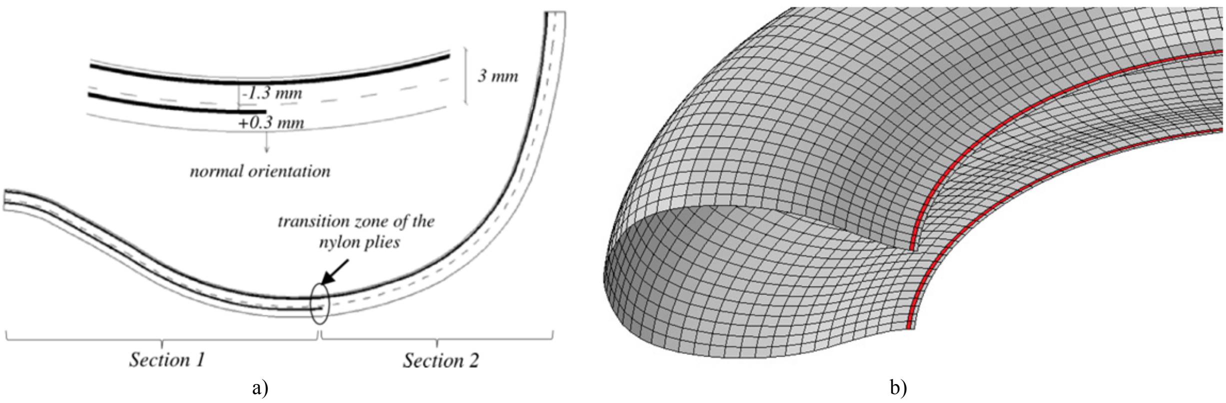

Fig. 5 Definition of rebar layers in the efficient shell model of the bias-ply tyre: a) Nylon cord plies and b) Steel bead wire

Table 2: Mesh properties for 3D models of the bias-ply tyre

	Segments in concentric direction	Number of elements
Solid model	90	95,115
	180	201,063
	720	794,397
Shell model	90	2,880
	180	10,440
	720	40,320

A compression test is performed on the tyre, using an INSTRON electromechanical testing bench. The tyre is inflated to 3.0 bar and placed between two rigid plates, as in Fig. 6a. The upper plate moves downward at a constant rate of 1.0 mm/min, while the force is measured. Three experiments were performed at this testing speed, for which the average force curve is shown in Fig. 7. The maximum standard deviation is 10.2 N.

The numerical model attempts to simulate compression of the tyre as close as possible to the experiment. The simulated tyre is also brought to 3.0 bar internal pressure and placed between two rigid plates. The frictional coefficient between the plates and the rubber is again assumed μ_f =0.7. The compression of the tyre is computed by the implicit solver ABAQUS/Standard. Fig. 6b shows the deformation of the detailed solid model with a 180 segments mesh.

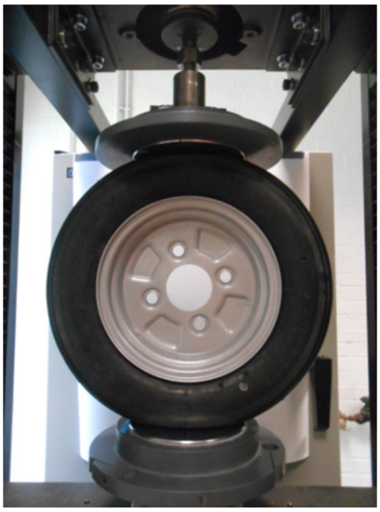

a)

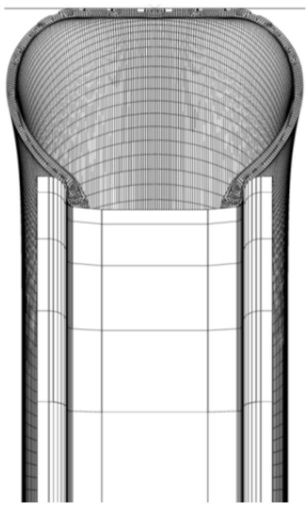

b)

Fig. 6 Compression test of bias-ply tyre at 1 mm/min: a) Experiment and b) Cut view of simulation.

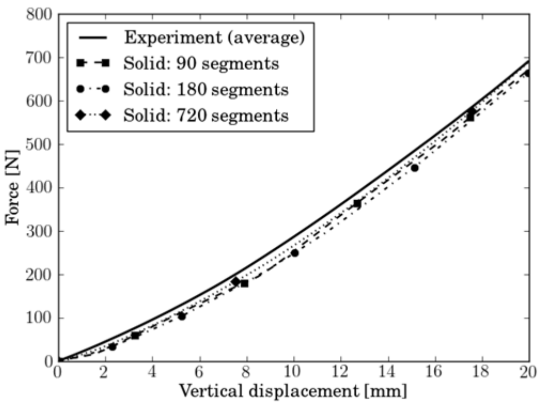

a)

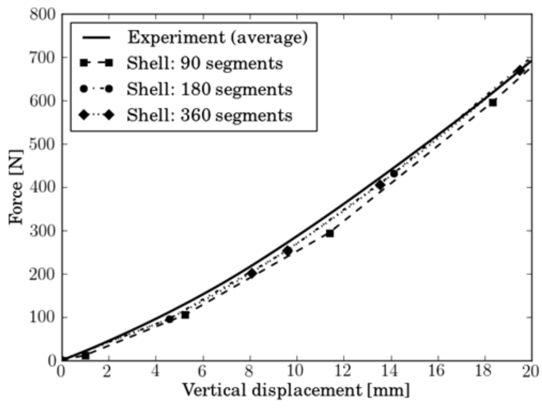

b)

Fig. 7 Force vs. displacement for compression test of the bias-ply tyre: mean experimental curve and simulated results for a) Solid models and b) Shell models.

The resulting force vs. displacement relations of Figure 7 show that both the detailed and efficient shell models with a sufficiently fine mesh correspond well to the experiment. The shell model with 180 segments is further used for impact simulation.

3. Impact against force and pressure plate

For validation of the numerical model, a number of experiments are conducted on the tempered glass calibration plate, as described by the standard EN 12600. Additional testing is performed by letting the pendulum impactor drop on a force plate and pressure plate setup, as a variation on the drop test against a rigid wall performed by Schneider (2001) and Müller de Vries (2012), but allowing for more detailed measurement of the impact.

3.1. Test setup

Force and pressure plate setups are more commonly used in the field of sports biomechanics. They are used in this study to measure the impact forces and to provide an image of the tyre footprint and its pressure distribution during contact. The force plate is of the type KISTLER 9281 B11 and has dimensions 0.6 x 0.4 x 0.1 m. It is characterized by a high rigidity, implying minimal deflections, and is used in combination with an 8-channel charge amplifier Type 9865E. The force plate is connected to an electronic unit which converts the electrical charges yielded by the force transducers into electrical voltages. Eight transducers allow calculation of the in- and out-of-plane forces. The calibrated range of the vertical force lies between 0 and 20 kN. The pressure plate is a RSscan International Hi-End footscan system with dimensions 0.58 x 0.42 m. It consists of 4096 sensors, arranged in a 64 x 64 matrix, and sensor dimensions 7.62 x 5.08 mm. The measurable pressure range lies between 1 and 127 N/cm² and the maximum data acquisition frequency is 500 Hz.

The force and pressure plate are mounted to an already existing test rig, which is built as described by the European Standard EN 12600. The measurement plates are attached to a 9.8 mm thick steel plate, fixed to the backside of the rear clamping frame. The test setup then looks as in Fig. 8a. It should be noted that the impactor and the pressure plate are not in contact when the impactor is at rest. Instead, there exists a gap over a horizontal distance of 147 mm. Consequently, this needs to be taken into account in the numerical model as well.

a)

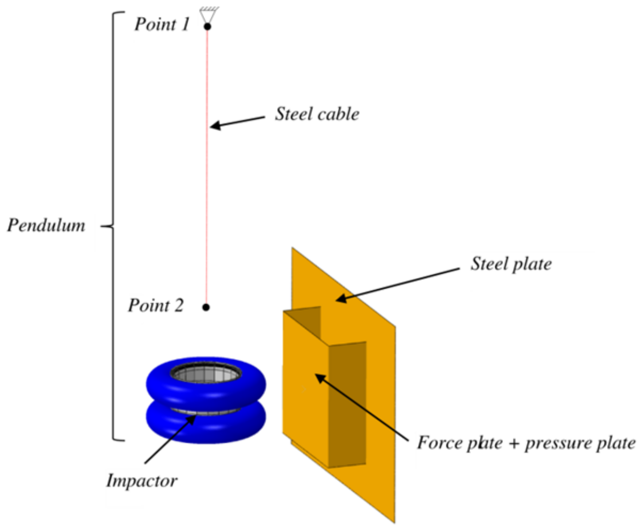

b)

Fig. 8 Twin-tyre pendulum impact setup with force and pressure plate: a) Photograph of experimental setup and b) FE model representation.

3.2. Numerical model

Figure 8b shows the finite element model of the impact test setup. The impactor consists of two tires and a steel cylinder, and has a total mass of 50 kg. Both tyre models consist of 10,440 elements, as described in Section 2.3. The inertia of the steel cylinder is allocated to a reference point in the gravitational centre of the steel cilinder. This reference point inside the impactor is coupled to Point 2 on Fig. 8b, where the impactor is hinged to a steel cable. Point 1 is at the location of the hinge that is connected to the frame, and its position is held fixed throughout the simulation. The steel cable is discretised by 1000 linear 2-node truss elements.

Both measurement plates and the steel plate to which they are connected are modelled as in Fig. 8b. The force and pressure plate are assumed rigid, while the steel plate cannot. During the tests, it was observed that the steel plate vibrates upon impact. Therefore, the steel plate is meshed by deformable shell elements and its vertical edges, which in reality are bolted to the frame, are assigned fixed boundary constraints.

The numerical analysis proceeds in two steps. First, the stresses and deformation of the tyres by inflation to 3.5 bar are calculated implicitly. Subsequently, the actual impact is simulated, in which the internal pressure and volume of the tyres is governed by the ideal gas equation of state Eq. 1 for air in the fluid cavities.

$$\rho(p,T) = \frac{p + p_a}{R(T - T_A)}, \tag{1}$$

where $\rho(p,T)$ is the fluid density at the current pressure and temperature, p_A the ambient pressure, p the gauge pressure and $p+p_A$ the absolute pressure. $R = 8.3144$ J/(K mol) is the universal gas constant, T the temperature and T_A is the absolute zero temperature.

At the start of the impact calculation, the pendulum impactor, then at its lowest point, is given an initial angular velocity ω_0. This velocity corresponds with the drop height and can be calculated by Eq. 2.

$$\omega = \sqrt{\frac{2gh}{L^2}}, \tag{2}$$

where h is the drop height, L the length from the fixed hinge to the centre of gravity of the impactor, and g is the gravitational constant. The gravitational acceleration is also taken into account during the impact simulation.

3.3. Comparison of simulation and test results

In Figure 9, the experimentally measured impact force is compared with the numerical result for different drop heights. Differences up to 11.1% and 13.5% are observed for the maximum force and corresponding impact time respectively, with an exception for a drop height of 20 mm. This deviation most likely has its origin in the experimental testing procedure. The positioning of the impactor to its correct drop height can only be realized with an accuracy of a few millimeters. For small drop heights, the error margin will therefore be larger. In Figure 10, the contact pressures are compared for impact from a drop height of 700 mm, at the time when the impact force peak is observed, i.e. $t = 24$ ms.

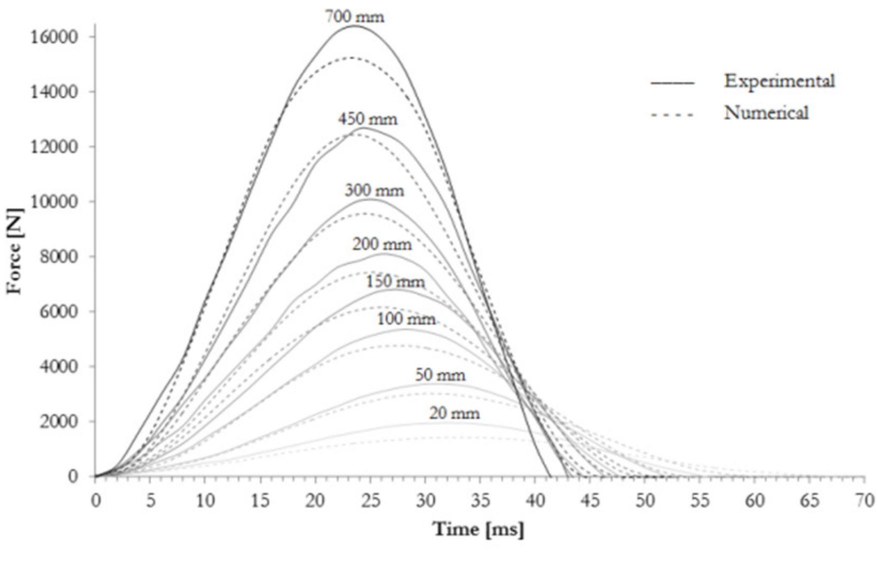

Fig. 9 Comparison of experimentally measured and simulated impact forces for different drop heights of the twin-tyre pendulum impactor.

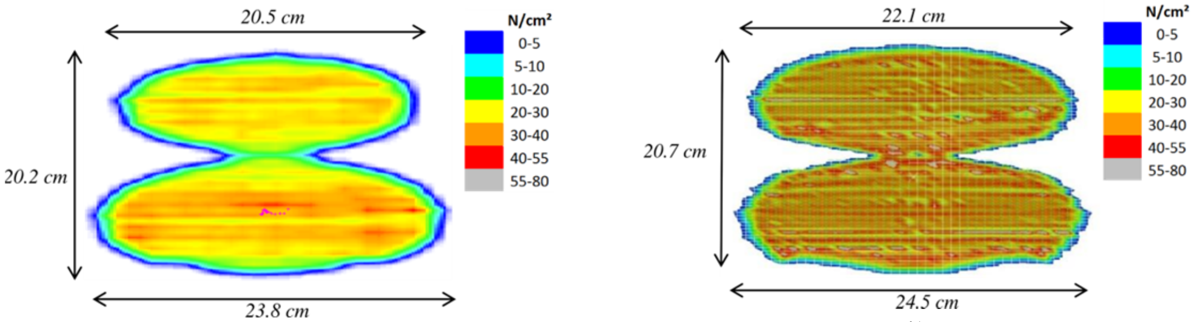

a) b)

Fig. 10 Comparison of tyre footprints for a drop height of 700 mm at t = 24.0 ms after impact at a drop height of 700 mm: a) Experimental measurement and b) Simulated result.

4. Impact on a laminated glass plate

This setup is described in fullness by the European Standard EN 12600 (2002). The test plate is a laminated soda lime silicate glass panel of dimensions 876 x 1938 mm with two glass plies of 3 mm thick and a 1.52 mm thick interlayer. The glass panel is clamped between two rigid, steel frames with a 20mm wide and 10 mm thick rubber lining with hardness of 57 IRHD. When clamped, the rubber strips are compressed by 10% of their thickness. The test rig is considered to be calibrated when the maximum strains upon impact, measured in the middle of the test plate, are within prescribed boundaries for each corresponding drop height. Impact testing is performed for drop heights up to 1200 mm. The mechanical properties of the glass are: Young's modulus $E = 70$ GPa, Poisson ratio ν = 0.23 and density ρ = 2500 kg/m³. The PVB is of the type Saflex R, manufactured by Eastman Chemical and has small-strain viscoelastic properties as given by D'haene and Savineau (2007).

The numerical model of the impactor used in these simulations has been described in Section 3.2. When the impactor is at rest, the tyre and glass plate are `just touching'. The glass plates are meshed by 5.0 x 5.0 mm shell elements which share nodes with two layers of solid elements for the PVB interlayer. The steel frames are considered rigid, and the 10 mm thick rubber strips are meshed with hexahedral continuum elements. The clamping of the glass plates by compression between the frames is simulated in a separate analysis step that precedes the impact simulation. In this step, both frames are moved towards each other, thus compressing the rubber strips by 10%. The rubber is characterised by a Mooney-Rivlin strain energy density function, with constants C_{10} = 0.417 MPa and C_{01} = 0.104 MPa, and bulk modulus K = 2 GPa.

Similarly, the pendulum impact is simulated using SJ MEPLA 3.5.9, which is a finite element software package specifically tailored to the needs of the civil engineering industry. This software includes a simplified manner of representing the impactor as a system of a mass and a spring. The spring stiffness C_R is given by Eq. 3 and was determined in the work of Schneider (2001).

$$C_R = 300 + 2\left|\Delta w_R\right|, \tag{3}$$

where Δw_R is the change in distance between the center of the mass and the contact point of the impactor. Furthermore, the laminated glass is simplified as a monolithic glass panel of the same thickness, which is a justified choice, because the interlayer acts rather stiff under such dynamic loading rate such that full transfer of shear stresses occurs. The clamped boundary conditions are represented by fixing the nodes at the edges of the glass panel in perpendicular direction to the surface.

Results of the simulations are compared to the experiments in Fig. 11 for a drop height of 450 mm. Fig. 12 gives the peak accelerations and peak strains for all simulated and tested drop heights. It is apparent that both simulations are conservative in that they consistently overpredict the accelerations and strains. For all cases considered, the detailed model in ABAQUS captures the impact behaviour marginally better than the model in SJ MEPLA. The modelling technique in SJ MEPLA is known to have been used in qualification in accordance with DIN 18008-4. This indicates that the detailed model may qualify this standard as well. Nevertheless, the difference in results between both simulations and the experiments is notable. The reason may lie in the controlling of the experimental setup for these particular tests, for which it is likely that the pressure in the tyres has not been as specified in the norm. However, the influence of tyre pressure is an aspect that needs further corroboration.

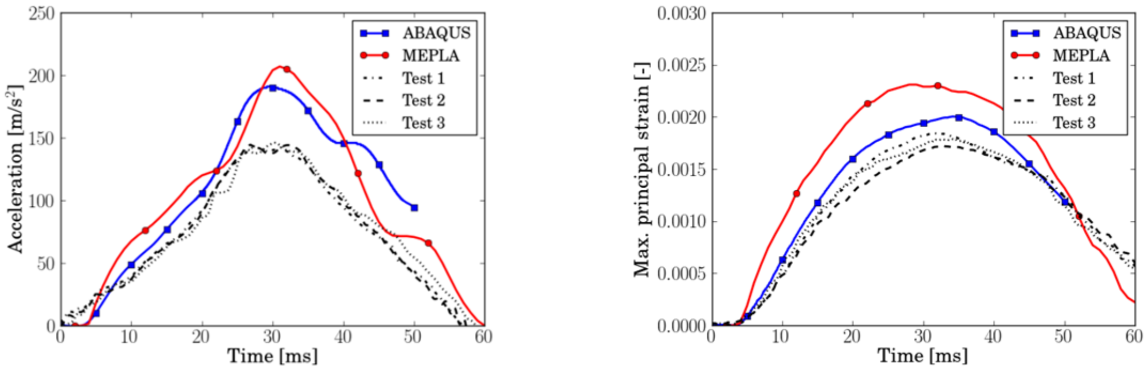

a) b)

Fig. 11 Response of laminated glass upon pendulum impact at a drop height of 450 mm: a) Accelerations and b) Strain.

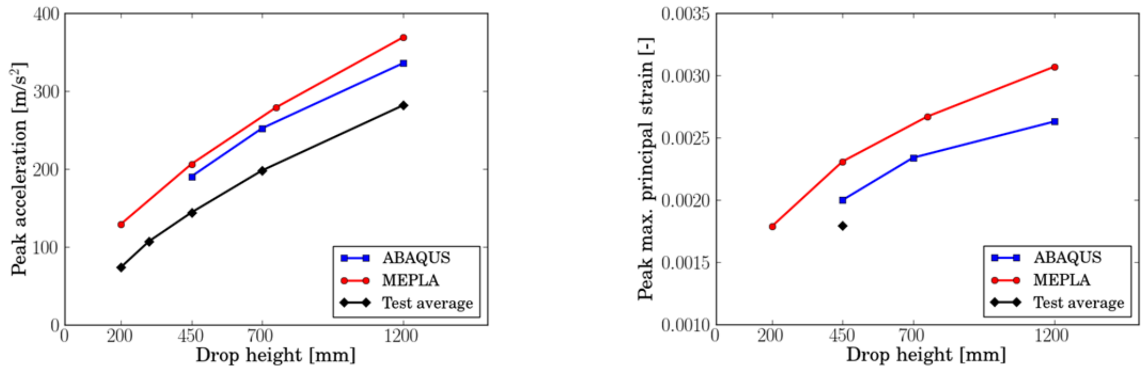

a) b)

Fig. 12 Peak values for response of laminated glass upon pendulum impact at various drop heights: a) Acceleration and b) Strain.

5. Conclusions and outlook

A detailed numerical model to simulate the twin-tyre pendulum impact test according to EN 12600 (2002) has been conceived. The model for the tyres accounts for the compressibility of the pressurised air volume within, and models the nylon reinforcements of the rubber material veraciously. Also the clamping conditions for the glass test plate are modelled realistically by statically compressing the rubber frame linings. The tyre model could be validated for both a compression test and for dynamic impact on a quasi-rigid pressure plate, showing good correspondence for the resulting forces as well as the contact footprint of the tyres.

Further experiments and simulations have been conducted on laminated glass plates from different drop heights. These results are also compared to simulations in SJ MEPLA, which offers a simplified modelling technique for the pendulum test and has been used for qualification to the German standard DIN 18008-4. Both simulation methods overpredict the accelerations and strains during the impact, which is conservative from a structural design point of view. The results of the detailed model are somewhat closer to the experimental data than those obtained with SJ MEPLA. But it can be concluded that qualification to the standard by simulation would benefit little from the detailed approach as described here, considering the effort required to build the model. However, the detailed model allows simulation of the glass breakage as well, thus providing a means to assess the post-breakage safety performance of laminated glass with a well-known and well-controlled test setup. This next step can be taken by modelling the laminated glass panel as in (Pelfrene et al., 2016a), combined with the crack delay model for glass, presented in (Pelfrene et al., 2016b).

Acknowledgements

The authors gratefully acknowledge AGC Glass Europe and Eastman Chemical for providing the laminated glass panels used for the experimental data presented in this work.

References

ANSI Z97.1: American National Standard for safety glazing materials used in buildings – Safety performance specifications and methods of test (1975)

Balkow, K., von Bock, H., Krewinkel, H., Rinkens, R.: Glas am Bau – Technischer Leitfaden. Deutsche Verlags-Anstalt, Stuttgart. (1980)

Brendler, S., Haufe, A., Ummenhofer, T.: A detailed numerical investigation of insulated glass subjected to the standard pendulum test. In: International Symposium on the Application of Architectural Glass, München, Germany (2004)

CEN EN 12600:2002: Glass in Building – Pendulum Test – Impact test method and classification for flat glass. Beuth, Berlin (2002)

D'haene, P., Savineau, G.: Mechanical properties of laminated safety glass – FEM study. In: Glass Performance Days 2007, Tampere, Finland. p.594-598 (2007)

DIN 18008-4: Glas im Bauwesen – Bemessungs- und Konstruktionsregeln – Teil 4: Zusatzanforderungen an absturzsichernde Verglasungen. Beuth, Berlin (2013)

ECE R-33: Uniform provisions concerning the approval of vehicles with regard to the behaviour of the structure of the impacted vehicle in a head-on collision. United Nations. (1993)

ECE R-94: Uniform provisions concerning the approval of vehicles with regard to the protection of the occupants of the impacted vehicle in a head-on collision. United Nations. (2002)

European Enhanced Vehicle-safety Committee: Working Group 17 Report: Improved test methods to evaluate pedestrian protection afforded by passenger cars. (1998)

Korunovic, N., Trajanovic, M., Stojkovic, M.: FEA of tyres subjected to static loading. J. Serb. Soc. Comp. Mech. 1, 87-98 (2007)

Liu, Q., Liu, J., Miao, Q., Wang, D., Tang, X.: Simulation and test validation of windscreen subjected to pedestrian head impact. In: 12th International LS-DYNA Users Conference. (2012)

Müller de Vries, C.: Numerical simulation of façade/window glazing fracture under impact loading. In: Proceedings of Challenging Glass 3, Ed.: Bos, F., Louter, C., Nijsse, R., Veer, F. p. 489-500 (2012)

Peng, Y., Yang, J., Deck, C., Willinger, R.: Finite element modelling of crash test behaviour for windshield laminated glass. Int. J. Imp. Engng. 57, 27-35 (2013)

Pelfrene, J., Kuntsche, J., Van Dam, S., Van Paepegem, W., Schneider, J.: Critical assessment of the post-breakage performance of blast loaded laminated glazing: experiments and simulations. Int. J. Imp. Engng. 88, 61-71 (2016a)

Pelfrene, J., Van Dam, S., Sevenois, R., Gilabert, F., Van Paepegem, W.: Fracture simulation of structural glass by element deletion in explicit FEM. In: Bos, F., Louter, C., Belis, J., editors. Challenging Glass Conference 5. (2016b)

Sang, Y., Dubé, M., Grant, M.: Dependence of friction on roughness, velocity and temperature. Phys. Rev. E 77, 036123 (2008)

Schneider, J.: Festigkeit und Bemessung punktgelagerter Gläser und stossbeanspruchter Gläser. Doctoral dissertation, Technische Universität Darmstadt, Germany (2001)

Schneider, J., Schula, S., Burmeister, A.: Zwei Verfahren zum rechnerischen Nachweis der dynamischen Beanspruchung von Verglasungen durch weichen Stoss, Teil 1: numerische, transiente Simulationsberechnung und vereinfachte Verfahren mit statischen Ersatzlasten. Stahlbau 80, 81-87 (2011)

Tabor, D.: The bulk modulus of rubber. Polymer 35(13), 2759-2763 (1994)

Timmel, M.: A finite element model for impact simulation with glass. Int. J. Imp. Engng. 34:1465-1478 (2007)

Technische Regeln für die Verwendung von absturzsichernden Verglasungen (TRAV). Deutsches Institut für Bautechnik (DIBt). Berlin (2003)

Zhao, S., Dharani, L.R., Chai, L., Barbat, S.: Analysis of damage in automotive glazing subjected to simulated head impact. Eng. Fail. Anal. 13:582-597 (2006)